Atmos. Chem. Phys., 15, 9521–9536, 2015
www.atmos-chem-phys.net/15/9521/2015/
doi:10.5194/acp-15-9521-2015

Atmospheric Chemistry and Physics
Open Access

Atmospheric isoprene ozonolysis: impacts of stabilised Criegee intermediate reactions with SO_2, H_2O and dimethyl sulfide

M. J. Newland[1,a], A. R. Rickard[2,3], L. Vereecken[4], A. Muñoz[5], M. Ródenas[5], and W. J. Bloss[1]

[1]University of Birmingham, School of Geography, Earth and Environmental Sciences, Birmingham, UK
[2]National Centre for Atmospheric Science (NCAS), University of York, York, UK
[3]Wolfson Atmospheric Chemistry Laboratories, Department of Chemistry, University of York, York, UK
[4]Max Planck Institute for Chemistry, Atmospheric Sciences, J.-J.-Becher-Weg 27, Mainz, Germany
[5]Instituto Universitario CEAM-UMH, EUPHORE Laboratories, Avda/Charles R. Darwin, Parque Tecnologico, Valencia, Spain
[a]now at: University of East Anglia, School of Environmental Sciences, Norwich, UK

Correspondence to: W. J. Bloss (w.j.bloss@bham.ac.uk) and A. R. Rickard (andrew.rickard@york.ac.uk)

Received: 9 March 2015 – Published in Atmos. Chem. Phys. Discuss.: 25 March 2015
Revised: 31 July 2015 – Accepted: 13 August 2015 – Published: 26 August 2015

Abstract. Isoprene is the dominant global biogenic volatile organic compound (VOC) emission. Reactions of isoprene with ozone are known to form stabilised Criegee intermediates (SCIs), which have recently been shown to be potentially important oxidants for SO_2 and NO_2 in the atmosphere; however the significance of this chemistry for SO_2 processing (affecting sulfate aerosol) and NO_2 processing (affecting NO_x levels) depends critically upon the fate of the SCIs with respect to reaction with water and decomposition. Here, we have investigated the removal of SO_2 in the presence of isoprene and ozone, as a function of humidity, under atmospheric boundary layer conditions. The SO_2 removal displays a clear dependence on relative humidity, confirming a significant reaction for isoprene-derived SCIs with H_2O. Under excess SO_2 conditions, the total isoprene ozonolysis SCI yield was calculated to be 0.56 ($\pm$0.03). The observed SO_2 removal kinetics are consistent with a relative rate constant, $k(\mathrm{SCI} + \mathrm{H_2O}) / k(\mathrm{SCI} + \mathrm{SO_2})$, of 3.1 ($\pm$0.5) $\times 10^{-5}$ for isoprene-derived SCIs. The relative rate constant for k(SCI decomposition) / k(SCI+SO_2) is 3.0 ($\pm$3.2) $\times 10^{11}$ cm^{-3}. Uncertainties are $\pm 2\sigma$ and represent combined systematic and precision components. These kinetic parameters are based on the simplification that a single SCI species is formed in isoprene ozonolysis, an approximation which describes the results well across the full range of experimental conditions. Our data indicate that isoprene-derived SCIs are unlikely to make a substantial contribution to gas-phase SO_2 oxidation in the troposphere. We also present results from an analogous set of experiments, which show a clear dependence of SO_2 removal in the isoprene–ozone system as a function of dimethyl sulfide concentration. We propose that this behaviour arises from a rapid reaction between isoprene-derived SCIs and dimethyl sulfide (DMS); the observed SO_2 removal kinetics are consistent with a relative rate constant, $k(\mathrm{SCI} + \mathrm{DMS}) / k(\mathrm{SCI} + \mathrm{SO_2})$, of 3.5 ($\pm$1.8). This result suggests that SCIs may contribute to the oxidation of DMS in the atmosphere and that this process could therefore influence new particle formation in regions impacted by emissions of unsaturated hydrocarbons and DMS.

1 Introduction

Atmospheric chemical processes exert a major influence on atmospheric composition. Identified gas-phase oxidants include the OH radical, ozone, NO_3 and under certain circumstances other species such as halogen atoms. Reactions with these oxidants can lead to (for example) chemical removal of primary air pollutants, formation of secondary pollutants (e.g. ozone, harmful to human and environmental health, and a greenhouse gas), and the transformation of gas-phase species to the condensed phase (e.g. SO_2 oxidation leading to the formation of sulfate aerosol, and the formation of func-

tionalised organic compounds leading to secondary aerosol formation, which can influence radiation transfer and climate).

Stabilised Criegee intermediates (SCIs), or carbonyl oxides, are formed in the atmosphere predominantly from the reaction of ozone with unsaturated hydrocarbons, though other processes may be important in certain conditions, e.g. alkyl iodide photolysis (Gravestock et al., 2010), dissociation of the dimethyl sulfoxide (DMSO) peroxy radical (Asatryan and Bozzelli, 2008), and reactions of peroxy radicals with OH (Fittschen et al., 2014). SCIs have been shown in laboratory experiments and by theoretical calculations to oxidise SO_2 and NO_2 (e.g. Cox and Penkett, 1971; Welz et al., 2012; Taatjes et al., 2013; Ouyang et al., 2013; Stone et al., 2014) as well as a number of other trace gases found in the atmosphere. Recent field measurements in a boreal forest (Mauldin III et al., 2012) and at a coastal site (Berresheim et al., 2014) have both identified an apparently missing process oxidising SO_2 to H_2SO_4 (in addition to reaction with OH) and have implied SCIs as a possible oxidant, acting alongside OH. Assessment of the importance of SCIs for tropospheric processing requires a quantitative understanding of their formation yields and atmospheric fate – in particular, the relative importance of bimolecular reactions (e.g. with SO_2), unimolecular decomposition, and reaction with water vapour. Here we describe an experimental investigation into the formation and reactions of the SCIs derived from isoprene (the most abundant biogenic volatile organic compound (VOC)), formed through the ozonolysis process, which dominates atmospheric SCI production, and studied under boundary layer conditions to assess their potential contribution to tropospheric oxidation.

1.1 Stabilised Criegee intermediate kinetics

Ozonolysis-derived CIs are formed with a broad internal energy distribution, yielding both chemically activated and stabilised CIs. SCIs can have sufficiently long lifetimes to undergo bimolecular reactions with H_2O and SO_2, amongst other species. Chemically activated CIs may undergo collisional stabilisation to an SCI (Scheme 1), or unimolecular decomposition or isomerisation.

To date the majority of studies have focused on the smallest SCI, CH_2OO, because of the importance of understanding simple SCI systems (this species is formed in the ozonolysis of all terminal alkenes) and the ability to synthesise CH_2OO from alkyl iodide photolysis, with sufficient yield to probe its kinetics. However, the unique structure of CH_2OO (which prohibits isomerisation to a hydroperoxide intermediate) likely gives it a different reactivity and degradation mechanism to other SCIs (Johnson and Marston, 2008).

Recent experimental work (Berndt et al., 2014; Newland et al., 2015; Chao et al., 2015; Lewis et al., 2015) has determined the predominant atmospheric fate for CH_2OO to be reaction with water vapour. Some of these experiments

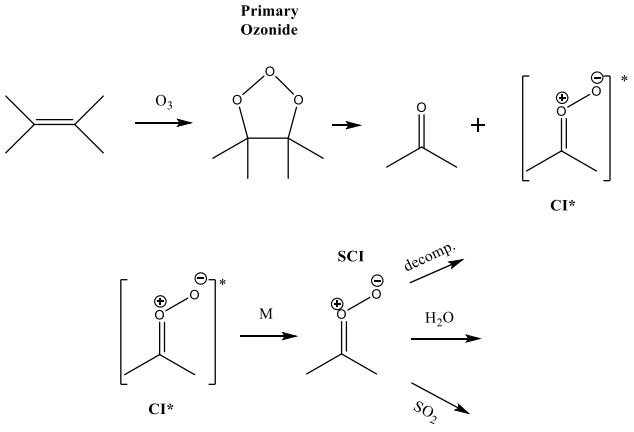

Scheme 1. Simplified generic mechanism for the reaction of Criegee intermediates (CIs) formed from alkene ozonolysis.

(Berndt et al., 2014; Chao et al., 2015; Lewis et al., 2015) have demonstrated a quadratic dependence of CH_2OO loss on $[H_2O]$, suggesting a dominant role for the water dimer, $(H_2O)_2$, in CH_2OO loss at typical atmospheric boundary layer H_2O concentrations. For larger SCIs, both experimental (Taatjes et al., 2013; Sheps et al., 2014; Newland et al., 2015) and theoretical (Kuwata et al., 2010; Anglada et al., 2011) studies have shown that their kinetics, in particular reaction with water, are highly structure dependent. *syn*-SCIs (i.e. those where an alkyl-substituent group is on the same side as the terminal oxygen of the carbonyl oxide moiety) react very slowly with H_2O, whereas *anti*-SCIs (i.e. with the terminal oxygen of the carbonyl oxide moiety on the same side as a hydrogen group) react relatively fast with H_2O. This difference has been predicted theoretically (Kuwata et al., 2010; Anglada et al., 2011) and was subsequently confirmed in recent experiments (Taatjes et al., 2013; Sheps et al., 2014) for the two CH_3CHOO conformers. Additionally, it has been predicted theoretically (Vereecken et al., 2012) that the relative reaction rate constants for the water dimer vs. water monomer, $k(\mathrm{SCI} + (H_2O)_2)/k(\mathrm{SCI} + H_2O)$ of larger SCIs (except *syn*-CH_3CHOO) will be over 70 times smaller than that for CH_2OO, suggesting that reaction with the water dimer is unlikely to be the dominant fate for these SCIs under atmospheric conditions.

An additional, and potentially important, fate of SCIs under atmospheric conditions is unimolecular decomposition (denoted k_d in Reaction R4). This is likely to be a significant atmospheric sink for *syn*-SCIs because of their slow reaction with water vapour. Previous studies have identified the hydroperoxide rearrangement as dominant for SCIs with a *syn* configuration, determining their overall unimolecular decomposition rate (Niki et al., 1987; Rickard et al., 1999; Martinez and Herron, 1987; Johnson and Marston, 2008). This route has been shown to be a substantial non-photolytic source of atmospheric oxidants (Niki et al., 1987; Alam et al.,

2013). CIs formed in the *anti* configuration are thought to primarily undergo rearrangement and possibly decomposition via a dioxirane intermediate ("the acid/ester channel"), producing a range of daughter products and contributing to the observed overall HO_x radical yield (Johnson and Marston, 2008; Alam et al., 2013).

For CH_2OO, rearrangement via a "hot" acid species represents the lowest accessible decomposition channel, with the theoretically predicted rate constant being rather low, $0.3\,s^{-1}$ (Olzmann et al., 1997). Recent experimental work supports this slow decomposition rate for CH_2OO (Newland et al., 2015; Chhantyal-Pun et al., 2015). However, Newland et al. (2015) suggest the decomposition of larger *syn*-SCIs to be considerably faster, albeit with substantial uncertainty, with reported rate constants for *syn*-CH_3CHOO of $288\,(\pm275)\,s^{-1}$ and for $(CH_3)_2COO$ of $151\,(\pm35)\,s^{-1}$. Novelli et al. (2014) estimated decomposition of *syn*-CH_3CHOO to be $20\,(3–30)\,s^{-1}$ from direct observation of OH formation, while Fenske et al. (2000) estimated decomposition of CH_3CHOO produced from ozonolysis of *trans*-but-2-ene to be $76\,s^{-1}$ (accurate to within a factor of 3).

$$\text{Alkene} + O_3 \xrightarrow{k_1} \phi\text{SCI} + (1-\phi)\text{CI} + \text{RCHO} \quad \text{(R1)}$$

$$\text{SCI} + SO_2 \xrightarrow{k_2} SO_3 + \text{RCHO} \quad \text{(R2)}$$

$$\text{SCI} + H_2O \xrightarrow{k_3} \text{Products} \quad \text{(R3)}$$

$$\text{SCI} \xrightarrow{k_d} \text{Products} \quad \text{(R4)}$$

$$\text{SCI} + (H_2O)_2 \xrightarrow{k_5} \text{Products} \quad \text{(R5)}$$

1.2 Isoprene ozonolysis

Global emissions of biogenic VOCs have been estimated to be an order of magnitude greater, by mass, than anthropogenic VOC emissions (Guenther et al., 1995). The most abundant non-methane biogenic hydrocarbon in the natural atmosphere is isoprene (2-methyl-1,3-butadiene, C_5H_8), with global emissions estimated to be $594\,(\pm34)\,Tg\,yr^{-1}$ (Sindelarova et al., 2014). While the vast majority of these emissions are from terrestrial sources, there are also biogenic emissions in coastal and remote marine environments, associated with seaweed and phytoplankton blooms (Moore et al., 1994). Isoprene mixing ratios (as well as those of some monoterpenes) have been reported to reach hundreds of pptv (parts per trillion by volume) over active phytoplankton blooms in the marine boundary layer (Sinha et al., 2007; Yassaa et al., 2008), with the potential to impact local air quality (Williams et al., 2010).

Removal of isoprene from the troposphere is dominated by reaction with the OH radical during the day and reaction with the nitrate radical during the night (Calvert et al., 2000). The ozonolysis of isoprene is also a non-photolytic source of HO_x radicals (Atkinson et al., 1992; Paulson et al., 1997; Malkin et al., 2010), with measured yields of OH between 0.25 (Paulson et al., 1997) and 0.27 (Atkinson et al., 1992)

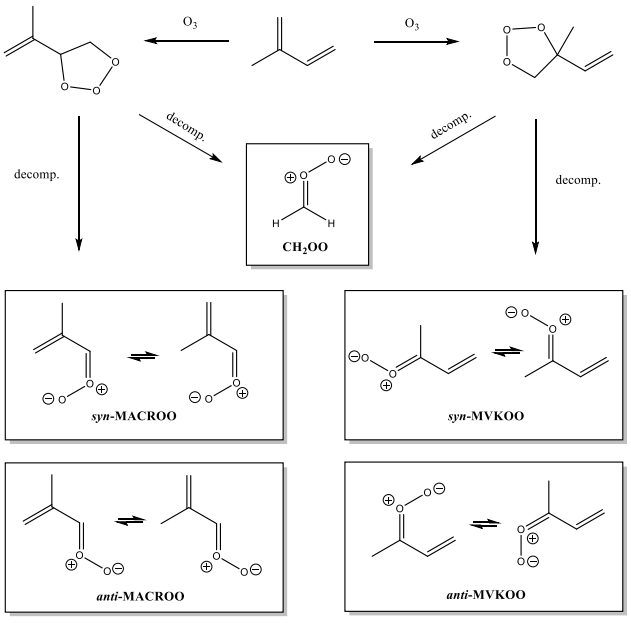

Scheme 2. Mechanism of formation of the nine possible Criegee intermediates (CIs) from isoprene ozonolysis.

(with a current recommended yield of 0.25; Atkinson et al., 2006). Isoprene ozonolysis also leads to the formation of a range of multi-functional oxygenated compounds, some of which can form secondary organic aerosol (Noziere et al., 2015).

Isoprene ozonolysis yields five different initial carbonyl oxides (Scheme 2). The three basic species formed are formaldehyde oxide (CH_2OO), methyl vinyl carbonyl oxide (MVKOO) and methacrolein oxide (MACROO) (Calvert et al., 2000; Atkinson et al., 2006). MVKOO and MACROO both have *syn* and *anti* conformers, and each of these can have either *cis* or *trans* configuration (Zhang et al., 2002; Kuwata et al., 2005) with easy inter-conversion between the *cis* and *trans* conformers (Aplincourt and Anglada, 2003). The kinetics and products of isoprene ozonolysis have been investigated theoretically by Zhang et al. (2002). They predicted the following SCI yields: CH_2OO, 0.31; *syn*-MVKOO, 0.14; *anti*-MVKOO, 0.07; *syn*-MACROO, 0.01; and *anti*-MACROO 0.04. This gives a total SCI yield of 0.57. They predicted that 95 % of the chemically activated CH_2OO formed will be stabilised, considerably higher than the experimentally determined stabilisation of excited CH_2OO formed during ethene ozonolysis (35–54 %) (Newland et al., 2015). This is because the majority of the energy formed during isoprene ozonolysis is thought to partition into the larger, co-generated, primary carbonyl species (Kuwata et al., 2005) (i.e. methyl vinyl ketone (MVK) or methacrolein (MACR)). The predicted stabilisation of the other SCIs ranges from 20 to 54 % at atmospheric pressure. It is relevant to note that the total SCI yield from isoprene ozonolysis used in the Master

Chemical Mechanism, MCMv3.2 (Jenkin et al., 1997; Saunders et al., 2003), is considerably lower at 0.22, as a consequence of the MCM protocol, which applies a weighted mean of total SCI yields measured for propene, 1-octene and 2-methyl propene (Jenkin et al., 1997). However, the relative yield of CH_2OO (0.50) compared to the total SCI yield in the MCM is very similar to that calculated by Zhang et al. (2002) (0.54).

1.3 Dimethyl sulfide (DMS)

The largest natural source of sulfur to the atmosphere is the biogenically produced compound dimethyl sulfide, DMS (CH_3SCH_3), which has estimated global emissions of $19.4\,(\pm 4.4)\,\mathrm{Tg\,yr^{-1}}$ (Faloona, 2009). DMS is a breakdown product of the plankton waste product dimethylsulfoniopropionate (DMSP). Jardine et al. (2015) have also recently shown that vegetation and soils can be important terrestrial sources of DMS to the atmosphere in the Amazon Basin, during both the day and at night, and throughout the wet and dry seasons, with measurements of up to 160 pptv within the canopy and near the surface. The oxidation of DMS is a large natural source of SO_2, and subsequently sulfate aerosol, to the atmosphere and is therefore an important source of new particle formation. This process has been implicated in an important feedback leading to a regulation of the climate in the pre-industrial atmosphere (Charlson et al., 1987). The two most important oxidants of DMS in the atmosphere are thought to be the OH and NO_3 radicals (Barnes et al., 2006) (Reactions R6 and R7). Because of its photochemical source, OH is thought to be the more important oxidant during the day in tropical regions, while NO_3 becomes more important at night, at high latitudes, and in more polluted air masses (Stark et al., 2007). Certain halogenated compounds, e.g. Cl (Wingenter et al., 2005) and BrO (Wingenter et al., 2005; Read et al., 2008), have also been suggested as possible oxidants for DMS in the marine environment.

$$\mathrm{DMS} + \mathrm{OH} \rightarrow \mathrm{CH_3SCH_2} + \mathrm{H_2O} \quad \text{(R6a)}$$
$$\rightarrow \mathrm{CH_3S(OH)CH_3} \quad \text{(R6b)}$$

$$\mathrm{DMS} + \mathrm{NO_3} \rightarrow \mathrm{CH_3SCH_2} + \mathrm{HNO_3} \quad \text{(R7)}$$

2 Experimental

2.1 Experimental approach

The EUPHORE facility is a $200\,\mathrm{m^3}$ simulation chamber used primarily for studying reaction mechanisms under atmospheric boundary layer conditions. Further details of the chamber setup and instrumentation are available elsewhere (Becker, 1996; Alam et al., 2011), and a detailed account of the experimental procedure, summarised below, is given in Newland et al. (2015).

Experiments comprised time-resolved measurement of the removal of SO_2 in the presence of the isoprene–ozone system, as a function of humidity or DMS concentration. SO_2 and O_3 abundance were measured using conventional fluorescence and UV absorption monitors, respectively; alkene abundance was determined via FTIR spectroscopy. Experiments were performed in the dark (i.e. with the chamber housing closed; $j(\mathrm{NO_2}) \leq 10^{-6}\,\mathrm{s^{-1}}$), at atmospheric pressure (ca. 1000 mbar) and temperatures between 287 and 302 K. The chamber is fitted with large horizontal and vertical fans to ensure rapid mixing (3 min). Chamber dilution was monitored via the first-order decay of an aliquot of SF_6, added prior to each experiment. Cyclohexane (ca. 75 ppmv) was added at the beginning of each experiment to act as an OH scavenger, such that SO_2 reaction with OH was calculated to be $\leq 1\,\%$ of the total chemical SO_2 removal in all experiments.

Experimental procedure, starting with the chamber filled with clean air, comprised addition of SF_6 and cyclohexane, followed by water vapour (or DMS), O_3 (ca. 500 ppbv) and SO_2 (ca. 50 ppbv). A gap of 5 min was left prior to addition of isoprene to allow complete mixing. The reaction was then initiated by addition of the isoprene (ca. 400 ppbv), and reagent concentrations followed for 30–60 min; typically ca. 25 % of the isoprene was consumed after this time. Nine isoprene + O_3 experiments, as a function of $[H_2O]$, were performed over separate days. Each individual run was performed at a constant humidity, with humidity varied to cover the range of $[H_2O] = 0.4\text{–}21 \times 10^{16}\,\mathrm{molecules\,cm^{-3}}$, corresponding to a relative humidity (RH) range of 0.5–27 % (at 298 K). Five isoprene + O_3 experiments as a function of DMS were also performed. Measured increases in $[SO_2]$ agreed with measured volumetric additions across the SO_2, humidity and DMS ranges used in the experiments.

2.2 Analysis

As in our previous study (Newland et al., 2015), from the chemistry presented in Reactions (R1)–(R5) SCIs will be produced in the chamber from the reaction of the alkene with ozone at a given yield, φ. A range of different SCIs are produced from the ozonolysis of isoprene (see Scheme 2: nine first-generation SCIs present), each with their own distinct chemical behaviour (i.e. yields, reaction rates). It is not feasible (from these experiments) to obtain data for each SCI independently; consequently, for analytical purposes we adopt two alternative analyses to treat the SCI population in a simplified (lumped) manner:

In the first of these, we make the approximation that all SCIs may be considered as a single species (defined from now on as ISOP-SCI). Alternatively, the SCI population is grouped into two species, the first of which is CH_2OO (for which the kinetics are known) and the second (hereafter termed CRB-SCI) represents all isomers of the other SCI species produced, i.e. Σ(MVKOO + MACROO). The im-

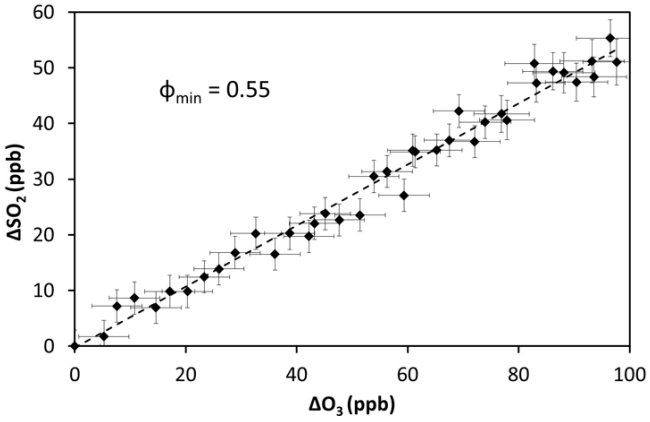

Figure 1. ΔSO_2 vs. ΔO_3 during the excess SO_2 experiments ($[H_2O] < 5 \times 10^{15}$ cm^{-3}). The gradient determines the minimum SCI yield (φ_{min}) from isoprene ozonolysis.

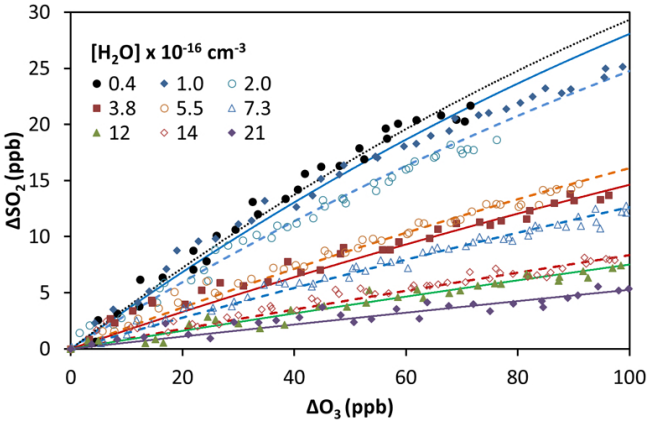

Figure 2. Cumulative consumption of SO_2 and O_3, ΔSO_2 versus ΔO_3, for the ozonolysis of isoprene in the presence of SO_2 at a range of water vapour concentrations, from 4×10^{15} to 2.1×10^{17} cm^{-3}. Symbols are experimental data corrected for chamber dilution. Lines are smoothed fits to the experimental data.

plications of these assumptions are discussed further below, but a key consequence is that the relative rate constants obtained from the analysis presented here are not representative of the elementary reactions of any single specific SCI isomer formed but rather represent a quantitative ensemble description of the integrated system, under atmospheric boundary layer conditions, which may be appropriate for atmospheric modelling.

Following formation in the ozonolysis reaction, the SCIs can react with SO_2, with H_2O, with DMS (if present), or with other species, or undergo unimolecular decomposition, under the experimental conditions applied. The fraction of the SCIs produced that reacts with SO_2 (f) is determined by the SO_2 loss rate ($k_2[SO_2]$) compared to the sum of the total loss processes of the SCIs (Eq. 1) :

$$f = \frac{k_2[SO_2]}{k_2[SO_2] + k_3[H_2O] + k_d + L} \quad (1)$$

Here, L accounts for the sum of any other chemical loss processes for SCIs in the chamber, after correction for dilution, and neglecting other (non-alkene) chemical sinks for O_3, such as reaction with HO_2 (also produced directly during alkene ozonolysis; Alam et al., 2013; Malkin et al., 2010), which was indicated through model calculations to account for < 0.5 % of ozone loss under all the experimental conditions.

2.2.1 SCI yield calculation

The value for the total SCI yield of ISOP-SCI, $\varphi_{ISOP\text{-}SCI}$, was determined from an experiment performed under dry conditions (RH < 1 %) in the presence of excess SO_2 (ca. 1000 ppbv), such that SO_2 scavenged the majority of the SCIs (> 95 %). From Eq. (2), regressing dSO_2 against dO_3 (corrected for chamber dilution), assuming f to be unity (i.e. all the SCIs produced reacts with SO_2), determines the value of φ_{min}, a lower limit to the SCI yield. Figure 1 shows the experimental data, from which φ_{min} was derived.

$$\frac{d[SO_2]}{d[O_3]} = \phi \cdot f \quad (2)$$

The lower-limit criterion applies because in reality f will be less than 1, at experimentally accessible SO_2 levels, as a small fraction of the SCIs will still react with trace H_2O present or undergo decomposition. The actual yield, $\varphi_{ISOP\text{-}SCI}$, was determined by combining the result from the excess-SO_2 experiment with those results from the series of experiments performed at lower SO_2, as a function of $[H_2O]$, to determine k_3/k_2 and k_d/k_2 (see Sect. 2.2.2) through an iterative process to determine the single unique value of $\varphi_{ISOP\text{-}SCI}$ which fits both data sets.

2.2.2 $k(SCI+H_2O)/k(SCI+SO_2)$ and $k_d/k(SCI+SO_2)$

By rearranging Eq. (1), the following equation (Eq. 3) can be derived. Therefore, in order to determine the relative rate constants k_3/k_2 and $(k_d+L)/k_2$, a series of experiments were performed in which the SO_2 loss was monitored as a function of $[H_2O]$ (see Sect. 2.1).

$$[SO_2]\left(\frac{1}{f} - 1\right) = \frac{k_3}{k_2}[H_2O] + \frac{k_d + L}{k_2} \quad (3)$$

From Eq. (2), regression of the loss of ozone (dO_3) against the loss of SO_2 (dSO_2) for an experiment at a given RH determines the product $f \cdot \varphi$ at a given point in time. This quantity will vary through the experiment as SO_2 is consumed, and other potential SCI co-reactants are produced, as predicted by Eq. (1). A smoothed fit was applied to the experimental data for the cumulative consumption of SO_2

and O_3, ΔSO_2 and ΔO_3 (as shown in Fig. 2), to determine dSO_2/dO_3 (and hence $f \cdot \varphi$) at the start of each experiment, for use in Eq. (3). This fit was derived using a box model run in FACSIMILE (Curtis and Sweetenham, 1987) with a chemical scheme taken from MCMv3.2 (http://mcm.leeds.ac.uk/MCM), with additional updated SCI chemistry constrained by the experimental measurements. The start of each experiment (i.e. when $[SO_2] \sim 50$ ppbv) was used as this corresponds to the greatest rate of production of the SCIs, and hence largest experimental signals (i.e. O_3 and SO_2 rate of change; greatest precision) and is the point at which the SCI + SO_2 reaction has the greatest magnitude compared with any other potential loss processes for either reactant species (see discussion below). The value $[SO_2]((1/f)-1)$ can then be regressed against $[H_2O]$ for each experiment to give a plot with a gradient of k_3/k_2 and an intercept of $(k_d + L)/k_2$ (Eq. 3). Our data cannot determine absolute rate constants (i.e. values of k_2, k_3, k_d) in isolation but are limited to assessing their relative values, which may be placed on an absolute basis through use of an (external) reference value ($k_2(CH_2OO + SO_2)$ in this case).

2.2.3 k(SCI+DMS)/k(SCI+SO_2)

A similar methodology was applied to that detailed in Sect. 2.2.2 to determine the relative reaction rate of ISOP-SCI with DMS $k(\text{SCI+DMS})/k(\text{SCI+SO}_2)$, k_8/k_2. Here, the SO_2 loss was determined as a function of [DMS] rather than $[H_2O]$. $[H_2O]$ was $< 1 \times 10^{16}$ molecules cm^{-3} for all experiments.

$$\text{SCI} + \text{DMS} \xrightarrow{k_8} \text{Products} \quad \text{(R8)}$$

Equation (3) is modified to give Eq. (4) by the addition of the DMS term. The gradient of a plot regressing $[SO_2]((1/f)-1)$ against [DMS] is then k_8/k_2 and the intercept is $k_3/k_2[H_2O] + (k_d + L)/k_2$. Using this intercept, these experiments can also be used to validate the k_3/k_2 and $(k_d+L)/k_2$ values derived from the experiments described in Sect. 2.2.

$$[SO_2]\left(\frac{1}{f}-1\right) = \frac{k_8}{k_2}[\text{DMS}] + \frac{k_3}{k_2}[H_2O] + \frac{k_d + L}{k_2} \quad (4)$$

3 Isoprene + ozone as a function of $[H_2O]$

3.1 SCI yield

Figure 1 shows the derived φ_{min} for isoprene, 0.55, determined from fitting Eq. (2) to the experimental data. φ_{min} was then corrected (< 3 %) as described in Sect. 2.2.1 using the k_3/k_2 and k_d/k_2 values determined from the measurements shown in Fig. 3 using Eq. (5). The corrected yield, $\varphi_{ISOP\text{-}SCI}$, is 0.56 (±0.03). Uncertainties are $\pm 2\sigma$ and represent the combined systematic (estimated measurement uncertainty) and precision components.

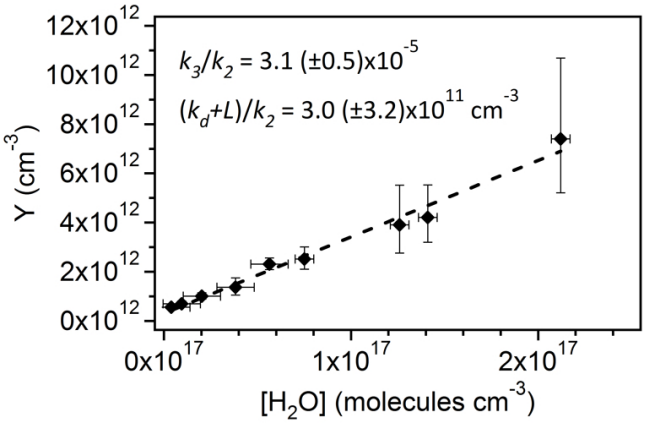

Figure 3. Application of Eq. (5) to derive relative rate constants for reaction of the isoprene-derived SCIs with H_2O (k_3/k_2) and decomposition ($(k_d+L)/k_2$). $Y = [SO_2]((1/f)-1) - k_9[\text{acid}]/k_2$.

Literature yields for SCI production from isoprene ozonolysis are given in Table 1. The value derived for the yield in this work agrees very well with the value of 0.58 (±0.26) from a recent experimental study (Sipilä et al., 2014) which used a similar single-SCI analysis approach.

Earlier experimental studies have reported lower values (by up to a factor of 2) for the total isoprene SCI yield. Rickard et al. (1999) derive a total yield of 0.28 from the increase in primary carbonyl yield (MVK and MACR) in the presence of a suitable SCI scavenger (excess SO_2). However, owing to the fact that they could not measure a formaldehyde yield, in their analysis it was assumed that 40 % of the chemically activated CH_2OO formed was stabilised (derived from the measured CH_2OO SCI yield for ethene ozonolysis), corresponding to their determination of a CH_2OO SCI yield of 0.18 for isoprene ozonolysis. If it is assumed that 95 % of the CH_2OO formed was actually stabilised, as calculated by Zhang et al. (2002), then this yield increases to 0.43, giving a total yield, $\varphi_{ISOP\text{-}SCI}$, of 0.53, in excellent agreement with the current work. Hasson et al. (2001) calculated a total SCI yield of 0.26 by measuring the sum of the difference between (i) the H_2O_2 production under dry and high-RH conditions (to give the non-CH_2OO SCI yield) and (ii) the difference between hydroxymethyl hydroperoxide (HMHP) production under dry and high-RH conditions (to give φ_{CH_2OO}). One potential reason for the significantly lower total SCI yield calculated by Hasson et al. compared to this work is the low value of φ_{CH_2OO} determined, potentially due to HMHP losses. Neeb et al. (1997) determined a value for φ_{CH_2OO} approximately twice that determined by Hasson et al., using a similar methodology. This discrepancy may be owing to the fact that Hasson et al. do not account for the formation of formic acid, which is a degradation product of HMHP. From theoretical calculations, Zhang et al. (2002) predicted a yield of 0.31 for CH_2OO, the most basic SCI, 0.14 for *syn*-MVKOO, 0.07 for *anti*-MVKOO, 0.04 for *anti*-

Table 1. Total isoprene SCI yields derived in this work and reported in the literature.

$\varphi_{\text{ISOP-SCI}}$	Reference	Methodology
0.56 (±0.03)	This work	SO_2 loss
0.58 (±0.26)	Sipilä et al. (2014)	Formation of H_2SO_4
0.30 (φ_{CH_2OO})[a]	Neeb et al. (1997)	HMHP[b] yield
0.26	Hasson et al. (2001)	Sum of difference between HMHP and H_2O_2 yields at high/low [H_2O]
0.28	Rickard et al. (1999)	Assumes stabilisation of 40 % of CH_2OO produced + difference between MVK and MACR production at high/low [SO_2]
0.53	Rickard et al. (1999)	Assuming 95 % of CH_2OO is stabilised (after Zhang et al., 2002) + difference between MVK and MACR production at high/low [SO_2]
0.57	Zhang et al. (2002)	Theoretical
0.22	MCMv3.2[c]	Based on a weighted average of the yields for propene, 1-octene and 2-methyl propene.

Uncertainty ranges (±2σ, parentheses) indicate combined precision and systematic measurement error components for this work, and are given as stated for literature studies. All referenced experimental studies produced SCIs from C_5H_8 + O_3 and were conducted between 700 and 760 Torr. [a] Yield of stabilised CH_2OO only. [b] Hydroxymethyl hydroperoxide (a first-order product of $CH_2OO + H_2O$). [c] http://mcm.leeds.ac.uk/MCM/ (Jenkin et al., 1997).

MACROO and 0.01 for *syn*-MACROO. This gives a sum of SCI yields of 0.57, again in very good agreement with the overall value derived here. The MCM (Jenkin et al., 1997; Saunders et al., 2003) applies a $\varphi_{\text{ISOP-SCI}}$ of 0.22, based on the limited experimental data available at the time of its original release (Jenkin et al., 1997). Although this total value is slightly lower than the experimental measurements reported prior to the release of MCMv3.2 (i.e. Rickard et al., 1999; Hasson et al., 2001), the protocol uses a similar relative yield for stabilised CH_2OO (0.50) compared to the total SCI yield as reported by Zhang et al. (2002). A probable reason for the low SCI yields in the MCM is the assumption of low stabilisation of the chemically activated CI formed.

The CH_2OO yield (φ_{CH_2OO}) from isoprene ozonolysis derived in this work can be calculated by multiplying the total SCI yield (0.56) by the fraction of the total SCI yield predicted to be CH_2OO by Zhang et al. (2002) (0.54). This gives a yield of stabilised CH_2OO from this work of 0.30. This is in very good agreement with Neeb et al. (1997), who derived a yield of stabilised CH_2OO from isoprene ozonolysis of 0.30 by measuring HMHP (the product of $CH_2OO + H_2O$) formation.

3.2 Analysis 1: single-SCI (ISOP-SCI) treatment

Figure 2 shows the cumulative consumption of SO_2 relative to that of O_3, ΔSO_2 versus ΔO_3 (after correction for dilution), for each isoprene ozonolysis experiment as a function of [H_2O]. A fit to each experiment, which has the sole purpose of extrapolating the experimental data to evaluate dSO_2/dO_3 at $t = 0$ (start of each experimental run) for use in Eqs. (1)–(3), is also shown. This fit is derived using a box model run in FACSIMILE (Curtis and Sweetenham, 1987) as described in Sect. 2.2.2. The overall change in SO_2, ΔSO_2, is seen to decrease substantially with increasing humidity over a relatively narrow range of [H_2O] (0.4–21 $\times 10^{16}$ cm^{-3}). This trend is similar to that seen for smaller, structurally less complex alkene ozonolysis systems (Newland et al., 2015), and is as would be expected from the understood chemistry (Reactions R1–R5), as there is competition between SO_2, H_2O, and decomposition for reaction with the SCIs formed.

Other potential fates for SCIs under the experimental conditions presented here include reaction with other reactants/co-products: ozone (Kjaergaard et al., 2013; Vereecken et al., 2014; Wei et al., 2014), other SCIs (Su et al., 2014; Vereecken et al., 2014), carbonyl products (Taatjes et al., 2012), acids (Welz et al., 2014), or the parent alkene itself (Vereecken et al., 2014). Sensitivity analyses were performed using a box model run in FACSIMILE (Curtis and Sweetenham, 1987) with a chemical scheme taken from the MCM, with additional updated SCI chemistry. Based on reported reaction rates of ozonolysis products with SCIs, these analyses indicate that the only reaction partners likely to compete significantly with SO_2, H_2O or unimolecular decomposition under the experimental conditions applied here are organic acids (i.e. HCOOH and CH_3COOH); these formed during the experiments, at concentrations reaching up to 2.5×10^{12} cm^{-3}. All other potential co-reactants listed above were calculated to account for < 10 % (for the worst-case run) of the total SCI loss under the experimental conditions applied.

Model runs were performed in which a rate constant of 1.1×10^{-10} cm^3 s^{-1} was used for reaction between SCIs and formic and acetic acids (HCOOH, CH_3COOH), as given by Welz et al. (2014) for CH_2OO + HCOOH, together with an acid yield of 0.5 from the reactions of isoprene-derived SCI

species with water, which gave a good agreement with the experimentally determined acid yields measured by FTIR. The reduction in SO_2 loss between the model runs with the SCI + acid reaction included, and those without the reaction, varied between 7 and 17 %.

Equation (3) can be extended to explicitly account for the presence of acids by inclusion of a further term (Eq. 5). This requires a value for k_9/k_2, the ratio of the rate constants for SCI reactions with acids and with SO_2. Here, we employ a value of 3.0, derived from the mean of the recently reported rates of reaction of CH_2OO with HCOOH and CH_3COOH (Welz et al., 2014), and the rate constant for $CH_2OO + SO_2$ reported by Welz et al. (2012) – although in reality this term represents potential reaction of all SCIs present with multiple acid species. The acid concentrations are taken from FTIR measurements during the experiments.

$$\text{SCI} + \text{acid} \xrightarrow{k_9} \text{Products} \quad \text{(R9)}$$

$$[SO_2]\left(\frac{1}{f} - 1\right) - \frac{k_9}{k_2}[\text{Acid}] = \frac{k_3}{k_2}[H_2O] + \frac{k_d + L}{k_2} \quad (5)$$

Figure 3 shows a fit of Eq. (5) to the data shown in Fig. 2, giving a gradient of k_3/k_2 and an intercept of the (relative) rate of SCI decomposition $(k_d + L)/k_2$. The results are well described by the linear relationship (Eq. 5) across the full range of experimental conditions. This suggests that the analytical approach described – of treating the SCIs produced from isoprene ozonolysis as a single system – provides a good quantitative description of the ISOP-SCI / O_3 / H_2O / SO_2 system under atmospheric boundary layer conditions, and hence provides a good approximation for use in atmospheric modelling studies. Reaction with the water dimer is not considered in this analysis (see discussion below). From Fig. 3 it is apparent that the observations can be described well by a linear dependence on $[H_2O]$ across the full range of experimental conditions applied. However, the humidity levels accessible in these experiments were limited (constrained by the operational range of the FTIR retrievals), and $[H_2O]$ can range up to $\sim 1 \times 10^{18}$ cm^{-3} in the atmosphere; the derived relationship may work less well at these high RHs as the role of the water dimer becomes more important; this is considered further in Sect. 3.3 (below), in which the SCI mix formed during isoprene ozonolysis is separated into CH_2OO and the other SCIs formed.

From Fig. 3, the derived relative rate constant for reaction of ISOP-SCI with water vs. SO_2, k_3/k_2, is 3.1 ($\pm$0.5) $\times 10^{-5}$ (Table 2). Newland et al. (2015) recently reported a k_3/k_2 relative rate constant for CH_2OO of 3.3 ($\pm$1.1) $\times 10^{-5}$ using the same experimental approach as used in this study. The value derived for ISOP-SCI here is the same, within uncertainty, as that derived for CH_2OO, suggesting that the other SCIs formed during isoprene ozonolysis have a mean k_3/k_2 similar to that of CH_2OO.

No absolute values of k_2 (SCI+SO_2) have been measured for ISOP-SCI. However, Welz et al. (2012) obtained an absolute value of k_2 (298 K) for CH_2OO (3.9×10^{-11} cm^3 s^{-1}), using direct methods at reduced pressure (a few Torr). If this value is used as an approximation for the k_2 value of ISOP-SCI (at atmospheric pressure and ambient temperature), then a k_3 (ISOP-SCI + H_2O) value of 1.2 ($\pm$0.2) $\times 10^{-15}$ cm^3 s^{-1} is determined (assuming the reaction between ISOP-SCI and water vapour is dominated by reaction with the water monomer, rather than the dimer, as discussed above).

From Eq. (5), the intercept in Fig. 3 gives the term $(k_d + L)/k_2$. $(k_d + L)$ will be dominated by k_d under the experimental conditions applied and analysis extrapolation to the start of each experimental run; however, the possibility of other chemical loss processes (see below) dictates that the derived value for k_d is technically an upper limit. From Fig. 3, k_d/k_2 is determined to be 3.0 ($\pm$3.2) $\times 10^{11}$ cm^{-3} (Table 2). Using the k_2 value determined by Welz et al. (2012) to put k_d/k_2 on an absolute scale (as above for k_3) yields a k_d of ≤ 12 ($\pm$12) s^{-1}. Newland et al. (2015) recently determined k_d for CH_2OO to be ≤ 4.7 s^{-1}. This suggests that k_d for the non-CH_2OO SCIs within the ISOP-SCI family is relatively low, i.e. a few tens per second, and/or that CH_2OO dominates the ISOP-SCI population. The limited precision obtained for these k_d values reflects the uncertainty in the intercept of the regression analysis shown in Fig. 3.

Sipilä et al. (2014) recently reported a value of k_{loss}/k_2 for isoprene ozonolysis-derived SCIs, treated using a single-SCI approach, which is analogous to the value $(k_3[H_2O] + k_d)/k_2$ reported in this section. They derive a value of 2.5 ($\pm$0.1) $\times 10^{12}$ cm^{-3} at $[H_2O] = 5.8 \times 10^{16}$ cm^{-3}. From the k_3 and k_d values derived in the single-SCI analysis in this work (Table 2), we calculate a value of 2.1 ($\pm$0.6) $\times 10^{12}$ cm^{-3} at the same $[H_2O]$, in good agreement.

The results presented here suggest that while SCI- and conformer-specific identification is important to determine the product yields, it does not appear to be important when solely considering the combined effects of isoprene ozonolysis products on the oxidation of SO_2 under the experimental conditions applied.

3.3 Analysis 2: two-SCI species (CH_2OO + CRB-SCI) treatment

In the preceding section, the combined effects of the five SCIs initially produced during isoprene ozonolysis were treated as a single pseudo-SCI, ISOP-SCI. In this section an alternative approach is presented, in which the SCI family is split into two components. These are CH_2OO, for which the reaction rates with water and the water dimer have been quantified in recent experimental studies, and the sum of the MVKOO and MACROO SCI, denoted CRB-SCI.

To date, the effects of the water dimer, $(H_2O)_2$, have only been determined experimentally for CH_2OO (Berndt et al., 2014; Chao et al., 2015; Lewis et al., 2015; Newland et al., 2015). Theoretical calculations (Vereecken et al., 2012) predicted the significant effect of the water dimer compared to

Table 2. Isoprene-derived SCI relative and absolute rate constants derived in this work [a].

SCI	$10^5 k_3/k_2$	$10^{15} k_3$ ($cm^3\ s^{-1}$)	$10^{-11} k_d/k_2$ (cm^{-3})	k_d (s^{-1})	k_8/k_2	$10^{10} k_8$ ($cm^3\ s^{-1}$)
CH_2OO[b]	3.3 (±1.1)	1.3 (±0.4)	−2.3[c] (±3.5)	−8.8[c] (±13)		
ISOP-SCI	3.1 (±0.5)	1.2 (±0.2)	3.0 (±3.2)	12 (±12)	3.5 (±2.2)	1.4 (±0.7)
CRB-SCI	2.9 (±0.7)	1.1 (±2.7)	6.6 (±7.0)	26 (±27)		

Uncertainty ranges (±2σ, parentheses) indicate combined precision and systematic measurement error components. [a] Scaled to an absolute value using $k_2(CH_2OO) = 3.9 \times 10^{-11}\ cm^3\ s^{-1}$ (Welz et al., 2012). [b] From Newland et al. (2015). [c] Values are indistinguishable from zero within the measurement uncertainties.

the monomer for CH_2OO, but also that the ratio of the SCI + $(H_2O)_2$: SCI + H_2O rate constants, k_5/k_3, of the larger, more substituted SCIs, *anti*-CH_3CHOO and $(CH_3)_2COO$, are 2–3 orders of magnitude smaller than for CH_2OO (Vereecken et al., 2012). This would make the dimer reaction negligible at atmospherically accessible [H_2O] (i.e. $< 1 \times 10^{18}\ cm^{-3}$) for SCIs larger than CH_2OO. The results presented in Sect. 3.2 show that, under the single-SCI treatment of the isoprene ozonolysis SCI chemistry, a water-monomer-only approach is able to describe the experimental data. Hence the effect of the water dimer reaction on CRB-SCI is not considered in this analysis (the water dimer reaction is included for CH_2OO).

$$[SO_2]\left(\frac{1}{f}-1\right)-\frac{k_9}{k_2}[\text{Acid}] = \gamma^A\left(\frac{k_3^A[H_2O]+k_5^A[(H_2O)_2]+(k_d^A+L^A)}{k_2^A}\right) + \gamma^C\left(\frac{k_3^C[H_2O]+(k_d^C+L^C)}{k_2^A}\right) \quad (6)$$

where ^{A} denotes CH_2OO and ^{C} denotes CRB-SCI.

Figure 4 shows three fits, obtained using Eq. (6) and corresponding to different treatments for the reaction of CH_2OO with H_2O and with $(H_2O)_2$, to the measured data presented in Fig. 3. For all three scenarios, the relative contribution of the two SCI components to the total SCI yield (γ) was assumed to be $\gamma^A = 0.54$ and $\gamma^C = 0.46$, after Zhang et al. (2002). k_3^A/k_2^A is assumed to be 3.3×10^{-5} after Newland et al. (2015).

The solid red line in Fig. 4 is a linear fit to the data to determine k_3^C and k_d^C. The $CH_2OO + (H_2O)_2$ rate constant, k_5^A, was assumed to be zero to reduce the number of free parameters. This assumption is reasonable considering the apparent linear dependence of the presented measurements on [H_2O] across the full range of conditions applied. The linear fit determines a value of $k_3^C/k_2^A = 2.9\ (\pm 0.7) \times 10^{-5}$ and a value of $(k_d^C + L^C)/k_2^A(\text{CRB-SCI}) = 6.6\ (\pm 7.0) \times 10^{11}\ cm^{-3}$ (Table 2). Again, as for the single species analysis, the decomposition term is poorly constrained.

The dashed blue line fits Eq. (6) using the parameters derived above for CRB-SCI and the water dimer relative reaction rate for CH_2OO determined in Newland et al. (2015),

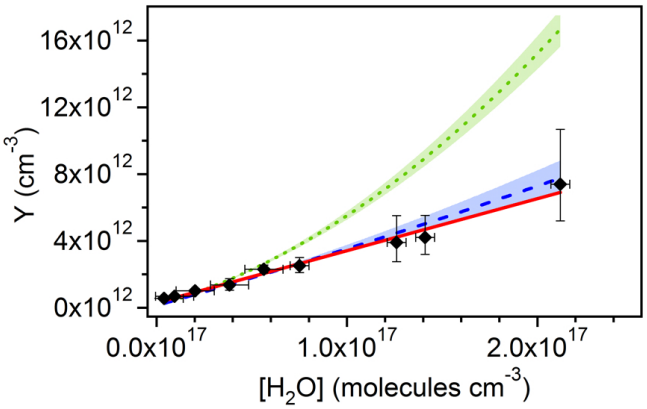

Figure 4. Application of Eq. (5) to derive relative rate constants for reaction of the sum of the MVKOO and MACROO SCI (CRB-SCI) with the water monomer, and the decomposition rate. Red line: water-monomer-only reactions; blue dashed line: water monomer reaction and CH_2OO water dimer reaction rate from Newland et al. (2015); green dotted line: CH_2OO water dimer reaction rate from Chao et al. (2015). Shaded areas indicate reported uncertainties on dimer reaction rates. $Y = [SO_2]((1/f) - 1) - k_9[\text{acid}]/k_2$.

$k_5/k_2 = 0.014\ (\pm 0.018)$. This still gives a good fit to the data in Fig. 4. The dotted green line is a similar fit but uses the recently directly determined $CH_2OO + (H_2O)_2$ rate, k_5^A, of $6.5\ (\pm 0.8) \times 10^{-12}\ cm^3\ s^{-1}$ by Chao et al. (2015). It is seen that this fit considerably overestimates the observations at higher [H_2O]. However, owing to the quadratic relationship of [$(H_2O)_2$] to [H_2O], a small difference in the rate constant can have a large effect, especially at higher [H_2O]. Possible explanations for this discrepancy are (i) that the kinetics observed for CH_2OO as formed from CH_2I_2 photolysis are not representative of the behaviour of the CH_2OO moiety as formed through alkene ozonolysis (although the conditions are such that a thermalised population would be expected in both cases); (ii) that the fraction of the total isoprene SCI yield that is CH_2OO is lower than that predicted by Zhang et al. (2002), and hence the effect of the $(H_2O)_2$ reaction overall is reduced – however, the predicted yield is in good agreement with those determined experimentally, albeit using indirect methods, so it seems unlikely that the actual CH_2OO yield is considerably lower; and (iii) that multiple effects are affecting the curvature of the results shown

in Fig. 4. Analogous plots for CH_3CHOO shown in Newland et al. (2015) displayed a shallowing gradient with increasing $[H_2O]$ (i.e. the opposite curvature to that caused by the $(H_2O)_2$ reaction). The probable explanation for the curvature observed for CH_3CHOO is the presence of a mix of *syn* and *anti* conformers (Scheme 2) in the system and the competing effects of the different kinetics of these two distinct forms of CH_3CHOO. A similar effect may arise for the isoprene-derived CRB-SCI which include multiple *syn* and *anti* conformers (see Scheme 2). The competition of this effect with that expected from the water dimer reaction may effectively lead to one masking the other under the experimental conditions applied.

Rate data for the reactions of isoprene-derived SCIs obtained using both analytical approaches described are given in Table 2.

3.4 Atmospheric implications

Treatment of the SCIs produced from isoprene ozonolysis as a single-SCI system appears to describe the observations well over the full range of experimental conditions accessible in this work (Sect. 3.2). The derived values for k_3(ISOP-SCI) reported here, obtained by fitting Eq. (5) to the measurements, placed on an absolute basis using the measured $k_2(CH_2OO + SO_2)$ of 3.9×10^{-11} cm^3 s^{-1}; Welz et al., 2012), corresponds to a loss rate for ISOP-SCI from reaction with H_2O in the atmosphere of 340 s^{-1} (assuming $[H_2O] = 2.8 \times 10^{17}$ molecules cm^{-3}, equivalent to an RH of 65 % at 288 K). Comparing this to the derived k_d value, 12 ($\pm$12) s^{-1}, it is seen that reaction with H_2O is predicted to be the main sink for isoprene-derived SCI in the atmosphere, with other sinks, such as decomposition and other bimolecular reactions, being negligible. Hence k_d is neglected in the following analysis.

An estimate of a mean steady-state ISOP-SCI concentration in the background atmospheric boundary layer can be calculated using Eq. (7).

$$[\text{ISOP}-\text{SCI}]_{ss} = \frac{[\text{Isoprene}][O_3]k_1\phi}{k_3[H_2O]} \quad (7)$$

Using the data given below, a steady-state SCI concentration of 4.1×10^2 molecules cm^{-3} is calculated for an isoprene ozonolysis source. This assumes an ozone mixing ratio of 40 ppbv, an isoprene mixing ratio of 1 ppbv, an SCI yield φ of 0.56, and a reaction rate constant k_1 (isoprene – ozone) of 1.0×10^{-17} cm^3 s^{-1} (288 K) (Atkinson et al., 2006), k_2 (ISOP-SCI + SO_2) of 3.9×10^{-11} cm^3 s^{-1}, and k_3 (ISOP-SCI + H_2O) of 1.2×10^{-15} cm^3 s^{-1}, and with $[H_2O]$ of 2.8×10^{17} cm^{-3} (RH $\sim$ 65 % at 288 K). A typical diurnal loss rate of SO_2 to OH (k_{OH}[OH]) is 9×10^{-7} s^{-1} (Welz et al., 2012), while the SO_2 loss rate arising from reaction with ISOP-SCI, using the values above, would be 1.6×10^{-8} s^{-1}. This suggests, for the conditions given above, the diurnally averaged loss of SO_2 to SCIs to be a very small fraction (1–2 %) of that due to OH. This analysis neglects additional chemical sinks for SCIs, which would reduce SCI abundance, and the possibility of other alkene ozonolysis products leading to SO_2 oxidation, which may increase the impact of alkene ozonolysis upon gas-phase SO_2 processing (Mauldin III et al., 2012; Curci et al., 1995; Prousek, 2009). However, the analysis also neglects additional sources of SCIs, e.g. photolysis of alkyl iodides (Gravestock et al., 2010; Stone et al., 2013), dissociation of the DMSO peroxy radical (Asatryan and Bozzelli, 2008; Taatjes et al., 2008), and reactions of peroxy radicals with OH (Fittschen et al., 2014), which are currently poorly constrained and may even dominate SCI production over an ozonolysis source in some environments.

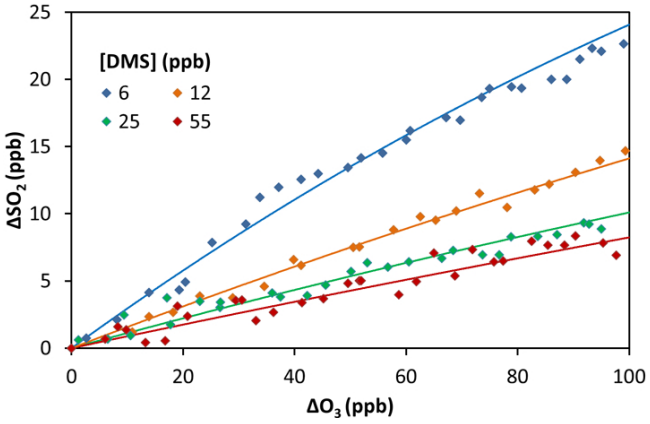

Figure 5. Cumulative consumption of SO_2 and O_3, ΔSO_2 versus ΔO_3, for the ozonolysis of isoprene in the presence of SO_2 at a range of DMS concentrations, from 6 to 55 ppbv. $[H_2O]$ in all experiments was $< 9 \times 10^{15}$ cm^{-3}. Markers are experimental data, corrected for chamber dilution. Solid lines are smoothed fits to the experimental data.

SCI concentrations are expected to vary greatly depending on the local environment, e.g. alkene abundance may be considerably higher (and with a different reactive mix of alkenes giving a range of structurally diverse SCIs) in a forested environment, compared to a rural background. Furthermore, isoprene emissions exhibit a diurnal cycle in forested environments owing to a strong temperature dependence; hence they are predicted to change significantly in the future as a response to a changing climate and other environmental conditions (Peñuelas and Staudt, 2010).

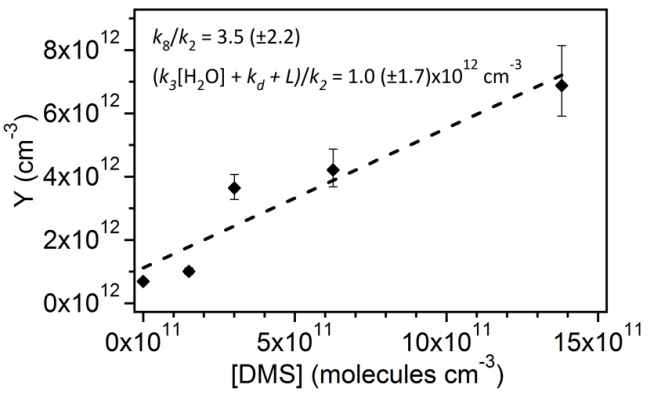

Figure 6. Application of Eq. (8) to derive rate constants for reaction of ISOP-SCI with DMS (k_8) relative to that for reaction with SO_2. $Y = [SO_2]((1/f) - 1) - k_9[\text{acid}]/k_2$.

4 Isoprene + ozone as a function of DMS

4.1 Results

A series of experiments analogous to those reported in Sect. 3 were performed as a function of dimethyl sulfide concentration, [DMS], rather than [H_2O]. Figure 5 shows that SO_2 loss in the presence of isoprene and ozone is increasingly inhibited by the presence of greater amounts of DMS. Under the experimental conditions applied, it is assumed that the SCIs produced in isoprene ozonolysis are reacting with DMS in competition with SO_2 (Reaction R8).

Equation (4) is analogous to Eq. (3) but for varying [DMS] rather than [H_2O]. However, as for the isoprene + O_3 as a function of water experiments described in Sect. 3, there is potential for the acid products of the isoprene ozonolysis reaction to provide an additional sink for SCIs in the chamber. Using the same methodology as described in Sect. 3.2, an explicit acid term was included in Eq. (4) to give Eq. (8).

$$[SO_2]\left(\frac{1}{f} - 1\right) - \frac{k_9}{k_2}[\text{Acid}] = \frac{k_8}{k_2}[\text{DMS}] + \frac{k_3}{k_2}[H_2O] + \frac{k_d + L}{k_2} \quad (8)$$

Figure 6 shows a fit of Eq. (8) to the experimental data. This yields a gradient of k_8/k_2 and an intercept of $(k_3[H_2O] + k_d + L)/k_2$. The derived relative rate constant of $k(\text{SCI+DMS})/k(\text{SCI+SO}_2)$, k_8/k_2, using this method is 3.5 (±1.8). Using the absolute value of $k_2(CH_2OO + SO_2)$ derived by Welz et al. (2012) (as described previously) determines a value of $k_8 = 1.4\ (\pm 0.7) \times 10^{-10}$ cm^3 s^{-1} (Table 2).

The intercept of the linear fit in Fig. 6 is 1.0 $(\pm 1.7) \times 10^{12}$ cm^{-3}. This represents $(k_3[H_2O] + k_d + L)/k_2$ and hence can also be compared with the kinetic parameters derived in Sect. 3 from the isoprene + O_3 as a function of H_2O experiments. From Fig. 3, $(k_d + L)/k_2 = 3.0\ (\pm 3.2) \times 10^{11}$ cm^{-3} and $k_3[H_2O]/k_2 = 2.5\ (\pm 0.4) \times 10^{11}$ cm^{-3} (with $[H_2O] = 8 \times 10^{15}$ cm^{-3}, the mean of the values for the five DMS experiments (6.7–8.8 $\times 10^{15}$ cm^{-3})), giving a combined value of 5.5 $(\pm 3.2) \times 10^{11}$ cm^{-3}. These two values therefore agree within the precision of the data.

4.2 Experimental uncertainties

As noted above, this analysis assumes that the multiple SCI species in reality present in the ozonolysis system may be analysed as a single species (or exhibit the same reactivity). While the data indicate that this approximation satisfactorily describes the observed behaviour under the conditions applied, other work (e.g. Taatjes et al., 2013) has shown that reactivity of different SCIs, and different conformers of the same SCIs, can differ, affecting the retrieval of kinetics in multi-SCI ozonolysis systems; Newland et al. (2015) illustrate this effect in the case of *syn*- and *anti*-CH_3CHOO. Similarly, the response of the SCI population to reaction with organic acids is approximated by a single reaction with those species observed (i.e. HCOOH, CH_3COOH). A further assumption made is that the mean isoprene–SCI + SO_2 reaction rate may be represented by that directly measured for CH_2OO with SO_2 (Welz et al., 2012). These approximations introduce systematic uncertainty into the derived rate constants, but given the lack of fundamental data for individual SCI isomers, it is not possible to evaluate this. The data obtained are well within the capability of the experimental approaches: DMS levels were inferred from the known volumetric addition to the chamber and are thought unlikely to be significantly in error. O_3 and isoprene were monitored using well-established techniques at levels well above their detection limits. The observed changes in SO_2 removal upon addition of DMS (as shown in Fig. 5) were substantial, well in excess of the sensitivity limit and uncertainty of the SO_2 monitor. However, it is important to note that no constraints regarding the products of the proposed DMS + SCI reaction were obtained; OH reaction with DMS is complex, proceeding through both abstraction and addition/complex formation channels, the latter rendered partially irreversible under atmospheric conditions through subsequent reaction with O_2 (Sander et al., 2011). The observed behaviour (Fig. 5) is not consistent with reversible complex formation dominating the SCI-DMS system under the conditions used; however it is possible that decomposition of such a complex to reform DMS, or its further reaction (e.g. with SO_2, analogous to the secondary ozonide mechanism proposed by Hatakeyama et al., 1986), would be consistent with the observed data, and also imply that the reaction may not lead to net DMS removal. Time-resolved laboratory measurements and product studies are needed to provide a test of this mechanistic possibility.

4.3 Discussion and atmospheric implications

To the authors' knowledge, this is the first work to show the relatively fast (in relation to other recently determined SCI bimolecular reactions, e.g. SCI + SO_2 and NO_2, and the well-established OH + DMS reaction) rate of reaction of SCIs with DMS, although the products have yet to be identified. While this work presents only SCIs derived from isoprene ozonolysis, it seems likely that the fast reaction rate will apply to all SCIs (though the precise rate will be structure-dependent).

DMS is mainly produced as a by-product of phytoplankton respiration, and so the highest concentrations are found in marine coastal environments or above active phytoplankton blooms. Furthermore, Jardine et al. (2015) recently showed that DMS mixing ratios within and above a primary Amazonian rainforest ecosystem can reach levels of up to 160 pptv, in canopy and above the surface, for periods of up to 8 h during the evening and into the night, with levels peaking at 80 pptv above canopy.

SCIs can also be expected to be present in the marine environment. As already discussed, mixing ratios of isoprene (Sinha et al., 2007; Yassaa et al., 2008) and monoterpenes (Yassaa et al., 2008) have been reported to reach in the region of hundreds of pptv over active phytoplankton blooms in the marine boundary layer. Additionally, the emission of small alkenes from coastal waters has been observed (Lewis et al., 1999). Furthermore, the photolysis of alkyl iodides (prevalent in the coastal environment; Jones et al., 2010) may be a significant source of SCIs (Stone et al., 2013). Berresheim et al. (2014) suggested that small SCIs derived from alkyl iodide photolysis may be responsible for observed H_2SO_4 production, in excess of that expected from measured SO_2 and OH concentrations, at the coastal atmospheric observatory Mace Head, Ireland. Jones et al. (2014) proposed SCIs produced from alkyl iodide photolysis as a possible source of surprisingly high formic acid concentrations observed in the marine environment in the European Arctic. Other non-ozonolysis sources of SCIs include dissociation of the DMSO peroxy radical (Asatryan and Bozzelli, 2008; Taatjes et al., 2008) (which could be an important source in the marine environment, where DMSO is an oxidation product of OH + DMS), and potentially from reactions of peroxy radicals with OH in remote atmospheres (Fittschen et al., 2014).

From the analysis in Sect. 3.4 a concentration of ISOP-SCI of 4.1×10^2 molecules cm^{-3} was calculated, assuming an isoprene concentration of 1 ppbv. In a remote marine environment isoprene concentrations are probably an order of magnitude lower than this, and consequently [ISOP-SCI] would be calculated to be on the order of 4×10^1 molecules cm^{-3}. However, some regions will be impacted by both high isoprene and DMS concentrations, for example tropical islands, such as Borneo, which can have high isoprene concentrations and are strongly influenced by marine air masses (MacKenzie et al., 2011), as well as significant terrestrial sources from vegetation and soils in the Amazon, especially into the evening and at night (Jardine et al., 2015), when ozonolysis chemistry is at its most effective relative to photochemical OH chemistry. High sulfate composition of organic aerosols collected from the Borneo rainforests likely arises from the chemical processing of oceanic emissions of DMS and SO_2 (Hamilton et al., 2013). The sulfate content of aerosols was observed to increase further over oil palm plantations in Borneo, where isoprene concentrations may reach levels on the order of tens of ppbv (MacKenzie et al., 2011), indicating scope for alkene ozonolysis–DMS chemical interactions to become significant. If a diurnally averaged [OH] is taken as 5×10^5 molecules cm^{-3}, then the loss rate of DMS to OH is $\sim 3.5 \times 10^{-6}$ s^{-1}, while the loss to ISOP-SCI, at a concentration of 1×10^2 cm^{-3}, is $\sim 2 \times 10^{-8}$ s^{-1}, i.e. about 0.4 % of the loss to OH. However in an environment with particularly high isoprene mixing ratios, such as over the oil palm plantations in Borneo, this could rise to a few percent.

SCIs derived from isoprene ozonolysis are unlikely to compete with OH during the daytime or NO_3 during the night, as an oxidant of DMS. However, alternative SCI sources have been suggested which may lead to significantly higher SCI concentrations in marine environments those predicted from ozonolysis alone. Further investigation is required to clarify the reasons for the observed discrepancies in SO_2 and DMS oxidation and the possibility that these may be, at least in part, explained by the presence of SCIs, dependent on the products of SCI–DMS interactions. SCIs are most likely of a similar importance to other minor reaction channels for DMS processing such as reaction with atomic chlorine or BrO, reported to have a reaction rate constant of $\sim 3.4 \times 10^{-10}$ cm^3 $molecule^{-1}$ s^{-1} at 298 K (Atkinson et al., 2004) and marine boundary layer concentrations on the order of 10^3–10^4 molecules cm^{-3} (von Glasow and Crutzen, 2007). SCIs may be most important for DMS oxidation during the evening period and early morning periods, when OH and NO_3 production are both relatively low.

5 Conclusions

Isoprene ozonolysis leads to gas-phase SO_2 removal, which decreases significantly with increasing water vapour. This trend is consistent with production of stabilised Criegee intermediates (SCIs) from the ozonolysis reaction, and the subsequent reaction of these species with SO_2 or H_2O. Competition between H_2O and SO_2 for reaction with the SCIs leads to this observed relationship, in which SCI abundance is sensitive to water vapour concentration, even at the dry end of the range found in the troposphere (ca. 1–20 % RH). The kinetics of this system can be described well by treatment of the SCI population as a single pseudo-SCI species under the experimental conditions applied, allowing for relatively

easy integration into atmospheric chemical models. The results indicate that SCIs derived from isoprene ozonolysis are unlikely to make a substantial contribution to atmospheric SO_2 oxidation and hence sulfate aerosol formation in the troposphere.

Furthermore, we show, for the first time, that SO_2 loss in the presence of isoprene and ozone significantly decreases with the addition of dimethyl sulfide (DMS). The data suggest a fast reaction of isoprene-derived SCIs with DMS. However, the exact mechanistic nature of the reaction, including the likely oxidation products, needs to be elucidated. This result has implications for the oxidation of DMS in the atmosphere. Although it seems unlikely that SCIs produced from isoprene ozonolysis alone are important for DMS oxidation, it is possible that (the sum of) SCI species produced from other alkene–ozone reactions, or from other (photo)chemical sources (which may be prevalent in the marine boundary layer), could be a significant source of DMS oxidant under certain atmospheric conditions and hence influence new particle formation above environments influenced by emissions of unsaturated hydrocarbons and DMS.

Acknowledgements. The assistance of the EUPHORE staff is gratefully acknowledged. Mat Evans, Salim Alam, Marie Camredon and Stephanie La are thanked for helpful discussions. This work was funded by EU FP7 EUROCHAMP-2 Transnational Access activity (E2-2012-05-28-0077), the UK NERC (NE/K005448/1) and Fundación CEAM. Fundación CEAM is partly supported by Generalitat Valenciana, and the project DESESTRES (Prometeo Program – Generalitat Valenciana). EUPHORE instrumentation is partly funded by the Spanish Ministry of Science and Innovation through the INNPLANTA project: PCT-440000-2010-003. Original data are available from the authors on request.

Edited by: S. A. Nizkorodov

References

Alam, M. S., Camredon, M., Rickard, A. R., Carr, T., Wyche, K. P., Hornsby, K. E., Monks, P. S., and Bloss, W. J.: Total radical yields from tropospheric ethene ozonolysis, Phys. Chem. Chem. Phys., 13, 11002–11015, 2011.

Alam, M. S., Rickard, A. R., Camredon, M., Wyche, K. P., Carr, T., Hornsby, K. E., Monks, P. S., and Bloss, W. J.: Radical Product Yields from the Ozonolysis of Short Chain Alkenes under Atmospheric Boundary Layer Conditions, J. Phys. Chem. A, 117, 12468–12483, 2013.

Anglada, J. M., Gonzalez, J., and Torrent-Sucarrat, M.: Effects of the substituents on the reactivity of carbonyl oxides. A theoretical study on the reaction of substituted carbonyl oxides with water, Phys. Chem. Chem. Phys., 13, 13034–13045, 2011.

Aplincourt, P. and Anglada, J. M.: Theoretical Studies on Isoprene Ozonolysis under Tropospheric Conditions, 1. Reaction of Substituted Carbonyl Oxides with Water, J. Phys Chem. A, 107, 5798–5811, 2003.

Asatryan, R. and Bozzelli, J. W.: Formation of a Criegee intermediate in the low-temperature oxidation of dimethyl sulfoxide, Phys. Chem. Chem. Phys., 10, 1769–1780, 2008.

Atkinson, R., Aschmann, S. M., Arey, J., and Shorees, B.: Formation of OH radicals in the gas-phase reaction of O_3 with a series of terpenes, J. Geophys. Res., 97, 6065–6073, 1992.

Atkinson, R., Baulch, D. L., Cox, R. A., Crowley, J. N., Hampson, R. F., Hynes, R. G., Jenkin, M. E., Rossi, M. J., and Troe, J.: Evaluated kinetic and photochemical data for atmospheric chemistry: Volume I – gas phase reactions of O_x, HO_x, NO_x and SO_x species, Atmos. Chem. Phys., 4, 1461–1738, doi:10.5194/acp-4-1461-2004, 2004.

Atkinson, R., Baulch, D. L., Cox, R. A., Crowley, J. N., Hampson, R. F., Hynes, R. G., Jenkin, M. E., Rossi, M. J., Troe, J., and IUPAC Subcommittee: Evaluated kinetic and photochemical data for atmospheric chemistry: Volume II – gas phase reactions of organic species, Atmos. Chem. Phys., 6, 3625–4055, doi:10.5194/acp-6-3625-2006, 2006.

Barnes, I., Hjorth, J., and Mihalopoulos, N.: Dimethylsulfide and dimethylsulfoxide and their oxidation in the atmosphere, Chem. Rev., 106, 940–975, 2006.

Becker, K. H.: EUPHORE: Final Report to the European Commission, Contract EV5V-CT92-0059, Bergische Universität Wuppertal, Germany, 1996.

Berndt, T., Voigtländer, J., Stratmann, F., Junninen, H., Mauldin III, R. L., Sipilä, M., Kulmala, M., and Herrmann, H.: Competing atmospheric reactions of CH_2OO with SO_2 and water vapour, Phys. Chem. Chem. Phys., 16, 19130–19136, 2014.

Berresheim, H., Adam, M., Monahan, C., O'Dowd, C., Plane, J. M. C., Bohn, B., and Rohrer, F.: Missing SO_2 oxidant in the coastal atmosphere? – observations from high-resolution measurements of OH and atmospheric sulfur compounds, Atmos. Chem. Phys., 14, 12209–12223, doi:10.5194/acp-14-12209-2014, 2014.

Calvert, J. G., Atkinson, R., Kerr, J. A., Madronich, S., Moortgat, G. K., Wallington, T. J., and Yarwood, G.: The Mechanism of Atmospheric Oxidation of the Alkenes, Oxford University Press, New York, USA, 552 pp., 2000.

Chao, W., Hsieh, J. -T., Chang C.-H., and Lin J. J. -M.: Direct kinetic measurement of the reaction of the simplest Criegee intermediate with water vapour, Science, 347, 751–754, doi:10.1126/science.1261549, 2015.

Charlson, R. J., Lovelock, J. E., Andreae, M. O., and Warren, S. G.: Oceanic phytoplankton, atmospheric sulphur, cloud albedo and climate, Nature, 326, 655–661, 1987.

Chhantyal-Pun, R., Davey, A., Shallcross, D. E., Percival, C. J., and Orr-Ewing, A. J.: A kinetic study of the CH_2OO Criegee intermediate self-reaction, reaction with SO_2 and unimolecular reaction using cavity ring-down spectroscopy, Phys. Chem. Chem. Phys., 17, 3617–3626, 2015.

Cox, R. A. and Penkett, S. A.: Oxidation of atmospheric SO_2 by products of the ozone-olefin reaction, Nature, 230, 321–322, 1971.

Curci, R., Dinoi, A., and Rubino, M. F.: Dioxirane oxidations: Taming the reactivity-selectivity principle, Pure Appl. Chem., 67, 811–822, 1995.

Curtis, A. R. and Sweetenham, W. P.: Facsimile/Checkmat User's Manual, Harwell Laboratory, Oxfordshire, 1987.

Faloona, I.: Sulfur processing in the marine atmospheric boundary layer: A review and critical assessment of modeling uncertainties, Atmos. Environ., 43, 2841–2854, 2009.

Fenske, J. D., Hasson, A. S., Ho, A. W., and Paulson, S. E.: Measurement of absolute unimolecular and bimolecular rate constants for CH_3CHOO generated by the trans-2-butene reaction with ozone in the gas phase, J. Phys. Chem. A, 104, 9921–9932, 2000.

Fittschen, C., Whalley, L. K., and Heard, D. E.: The reaction of CH_3O_2 radicals with OH radicals: a neglected sink for CH_3O_2 in the remote atmosphere, Environ. Sci. Technol., 48, 7700–7701, 2014.

Gravestock, T. J., Blitz, M. A., Bloss, W. J., and Heard, D. E.: A multidimensionsal study of the reaction CH_2I+O_2: Products and atmospheric implications, Chem. Phys. Chem., 11, 3928–3941, 2010.

Guenther, A., Hewitt, C. N., Erickson, D., Fall, R., Geron, C., Graedel, T., Harley, P., Klinger, L., Lerdau, M., McKay, W. A., Scholes, B., Steinbrecher, R., Tallamraju, R., Taylor, J., and Zimmerman, P.: A global model of natural volatile organic compound emissions, J. Geophys. Res., 100, 8873–8892, 1995.

Hamilton, J. F., Alfarra, M. R., Robinson, N., Ward, M. W., Lewis, A. C., McFiggans, G. B., Coe, H., and Allan, J. D.: Linking biogenic hydrocarbons to biogenic aerosol in the Borneo rainforest, Atmos. Chem. Phys., 13, 11295–11305, doi:10.5194/acp-13-11295-2013, 2013.

Hasson, A. S., Orzechowska, G., and Paulson, S. E.: Production of stabilized Criegee intermediates and peroxides in the gas phase ozonolysis of alkenes 1. Ethene, trans-2-butene, and 2,3-dimethyl-2-butene, J. Geophys. Res., 106, 34131–34142, 2001.

Hatakeyama, S., Kobayashi, H., Lin, Z.-Y., Takagi, H., and Akimoto, H.: Mechanism for the reaction of CH_2OO with SO_2, J. Phys. Chem., 90, 4131–4135, 1986.

Jardine, K., Yañez-Serrano, A. M., Williams, J., Kunert, N., Jardine, A., Taylor, T., Abrell, L., Artaxo, P., Guenther, A., Hewitt, C. N., House, E., Florentino, A. P., Manzi, A, Higuchi, N., Kesselmeier, J., Behrendt, T., Veres, P. R., Derstroff, B., Fuentes, J. D., Martin, S. T., and Andreae, M. O.: Dimethyl sulfide in the Amazon rain forest, Global Biogeochem. Cy., 29, 19–32, doi:10.1002/2014GB004969, 2015.

Jenkin, M. E., Saunders, S. M., and Pilling, M. J.: The tropospheric degradation of volatile organic compounds: a protocol for mechanism development, Atmos. Environ., 31, 81–104, 1997.

Johnson, D. and Marston, G.: The gas-phase ozonolysis of unsaturated volatile organic compounds in the troposphere, Chem. Soc. Rev., 37, 699–716, 2008.

Jones, B. T., Muller, J. B. A., O'Shea, S. J., Bacak, A., Le Breton, M., Bannan, T. J., Leather, K. E., Booth, A. M., Illingworth, S., Bower, K., Gallagher, M. W., Allen, G., Shallcross, D. E., Bauguitte, S. J. -B., Pyle, J. A., and Percival C. J.: Airborne measurements of HC(O)OH in the European Arctic: A winter – summer comparison, Atmos. Environ., 99, 556–567, 2014.

Jones, C. E., Hornsby, K. E., Sommariva, R., Dunk, R. M., von Glasow, R., McFiggans, G., and Carpenter, L. J.: Quantifying the contribution of marine organic gases to atmospheric iodine, Geophys. Res. Lett., 37, L18804, doi:10.1029/2010GL043990, 2010.

Kjaergaard, H. G., Kurtén, T., Nielsen, L. B., Jørgensen, S., and Wennberg, P. O.: Criegee Intermediates React with Ozone, J. Phys. Chem. Lett., 4, 2525–2529, 2013.

Kuwata, K. T., Valin, L. C., and Converse, A. D.: Quantum Chemical and Master Equation Studies of the Methyl Vinyl Carbonyl Oxides Formed in Isoprene Ozonolysis, J. Phys. Chem. A, 109, 10710–10725, 2005.

Kuwata, K. T., Hermes, M. R., Carlson, M. J., and Zogg, C. K.: Computational Studies of the Isomerization and Hydration Reactions of Acetaldehyde Oxide and Methyl Vinyl Carbonyl Oxide, J. Phys Chem. A, 114, 9192–9204, 2010.

Lewis, A. C., McQuaid, J. B., Carslaw, N., and Pilling, M. J.: Diurnal cycles of short-lived tropospheric alkenes at a north Atlantic coastal site, Atmos. Environ., 33, 2417–2422, 1999.

Lewis, T. R., Blitz, M. A., Heard, D. E., and Seakins, P. W.: Direct evidence for a substantive reaction between the Criegee intermediate, CH_2OO, and the water vapour dimer, Phys. Chem. Chem. Phys., 17, 4859–4863, 2015.

MacKenzie, A. R., Langford, B., Pugh, T. A. M., Robinson, N., Misztal, P. K., Heard, D. E., Lee, J. D., Lewis, A. C., Jones, C. E., Hopkins, J. R., Philips, G., Monks, P. S., Karunaharan, A., Hornsby, K. E., Nicolas-Perea, V., Coe, H., Whalley, L. K., Edwards, P. M., Evans, M. J., Stone, D., Ingham, T., Commane, R., Furneaux, K. L., McQuaid, J., Nemitz, E, Seng, Y. K., Fowler, D., Pyle, J. A., and Hewitt, C. N.: The atmospheric chemistry of trace gases and particulate matter emitted by different land uses in Borneo, Phil. Trans. R. Soc. B, 366, 3177–3195, 2011.

Malkin, T. L., Goddard, A., Heard, D. E., and Seakins, P. W.: Measurements of OH and HO_2 yields from the gas phase ozonolysis of isoprene, Atmos. Chem. Phys., 10, 1441–1459, doi:10.5194/acp-10-1441-2010, 2010.

Martinez, R. I. and Herron, J. T.: Stopped-flow studies of the mechanisms of alkene-ozone reactions in the gas-phase: tetramethylethylene, J. Phys. Chem., 91, 946–953, 1987.

Mauldin III, R. L., Berndt, T., Sipilä, M., Paasonen, P., Petäjä, T., Kim, S., Kurtén, T., Stratmann, F., Kerminen, V.-M., and Kulmala, M.: A new atmospherically relevant oxidant, Nature, 488, 193–196, 2012.

Moore, R. M., Oram, D. E., and Penkett, S. A.: Production of isoprene by marine phytoplankton cultures, Geophys. Res. Lett., 21, 2507–2510, 1994.

Neeb, P., Sauer, F., Horie, O., and Moortgat, G. K.: Formation of hydroxymethyl hydroperoxide and formic acid in alkene ozonolysis in the presence of water vapour, Atmos. Environ., 31, 1417–1423, 1997.

Newland, M. J., Rickard, A. R., Alam, M. S., Vereecken, L., Muñoz, A., Ródenas, M., and Bloss, W. J.: Kinetics if stabilised Criegee intermediates derived from alkene ozonolysis: reactions with SO_2, H_2O and decomposition under boundary layer conditions, Phys. Chem. Chem. Phys., 17, 4076–4088, 2015.

Niki, H., Maker, P. D., Savage, C. M., Breitenbach, L. P., and Hurley, M. D.: FTIR spectroscopic study of the mechanism for the gas-phase reaction between ozone and tetramethylethylene, J. Phys. Chem., 91, 941–946, 1987.

Novelli, A., Vereecken, L., Lelieveld, J., and Harder, H.: Direct observation of OH formation from stabilised Criegee intermediates, Phys. Chem. Chem. Phys., 16, 19941–19951, 2014.

Noziere, B., Kalberer, M., Claeys, M., Allan, J., D'Anna, B., Decesari, S., Finessi, E., Glasius, M., Grgić, I., Hamilton, J. F., Hoffmann, T., Iinuma, Y., Jaoui, M., Kahnt, A., Kampf, C. J., Kourtchev, I., Maenhaut, W., Marsden, N., Saarikoski, S., Schnelle-Kreis, J., Surratt, J. D., Szidat, S., Szmigielski, R.,

and Wisthaler, A.: The Molecular Identification of Organic Compounds in the Atmosphere: State of the Art and Challenges, Chem. Rev., 115, 3919–3983, doi:10.1021/cr5003485, 2015.

Olzmann, M., Kraka, E., Cremer, D., Gutbrod, R., and Andersson, S.: Energetics, Kinetics, and Product Distributions of the Reactions of Ozone with Ethene and 2,3-Dimethyl-2-butene, J. Phys. Chem. A, 101, 9421–9429, 1997.

Ouyang, B., McLeod, M. W., Jones, R. L., and Bloss, W. J.: NO_3 radical production from the reaction between the Criegee intermediate CH_2OO and NO_2, Phys. Chem. Chem. Phys., 15, 17070–17075, 2013.

Paulson, S. E., Chung, M., Sen, A. D., and Orzechowska, G.: Measurement of OH radical formation from the reaction of ozone with several biogenic alkenes, Geophys. Res. Lett., 24, 3193–3196, 1997.

Peñuelas, J., and Staudt, M.: BVOCs and global change, Trends Plant Sci., 15, 133–144, 2010.

Prousek, J.: Chemistry of Criegee Intermediates, Chem. Listy, 103, 271–276, 2009.

Read, K. A., Lewis, A. C., Bauguitte, S., Rankin, A. M., Salmon, R. A., Wolff, E. W., Saiz-Lopez, A., Bloss, W. J., Heard, D. E., Lee, J. D., and Plane, J. M. C.: DMS and MSA measurements in the Antarctic Boundary Layer: impact of BrO on MSA production, Atmos. Chem. Phys., 8, 2985–2997, doi:10.5194/acp-8-2985-2008, 2008.

Rickard, A. R., Johnson, D., McGill, C. D., and Marston, G.: OH Yields in the Gas-Phase reactions of Ozone with Alkenes, J. Phys. Chem. A, 103, 7656–7664, 1999.

Sander, S. P., Abbatt, J., Barker, J. R., Burkholder, J. B., Friedl, R. R., Golden, D. M., Huie, R. E., Kolb, C. E., Kurylo, M. J., Moortgat, G. K., Orkin, V. L., and Wine, P. H.: Chemical Kinetics and Photochemical Data for Use in Atmospheric Studies, Evaluation No. 17, JPL Publication 10-6, Jet Propulsion Laboratory, Pasadena, 2011

Saunders, S. M., Jenkin, M. E., Derwent, R. G., and Pilling, M. J.: Protocol for the development of the Master Chemical Mechanism, MCM v3 (Part A): tropospheric degradation of non-aromatic volatile organic compounds, Atmos. Chem. Phys., 3, 161–180, doi:10.5194/acp-3-161-2003, 2003.

Sheps, L., Scully, A. M., and Au, K.: UV absorption probing of the conformer-dependent reactivity of a Criegee intermediate CH_3CHOO, Phys. Chem. Chem. Phys., 16, 26701–26706, 2014.

Sindelarova, K., Granier, C., Bouarar, I., Guenther, A., Tilmes, S., Stavrakou, T., Müller, J.-F., Kuhn, U., Stefani, P., and Knorr, W.: Global data set of biogenic VOC emissions calculated by the MEGAN model over the last 30 years, Atmos. Chem. Phys., 14, 9317–9341, doi:10.5194/acp-14-9317-2014, 2014.

Sinha, V., Williams, J., Meyerhöfer, M., Riebesell, U., Paulino, A. I., and Larsen, A.: Air-sea fluxes of methanol, acetone, acetaldehyde, isoprene and DMS from a Norwegian fjord following a phytoplankton bloom in a mesocosm experiment, Atmos. Chem. Phys., 7, 739–755, doi:10.5194/acp-7-739-2007, 2007.

Sipilä, M., Jokinen, T., Berndt, T., Richters, S., Makkonen, R., Donahue, N. M., Mauldin III, R. L., Kurtén, T., Paasonen, P., Sarnela, N., Ehn, M., Junninen, H., Rissanen, M. P., Thornton, J., Stratmann, F., Herrmann, H., Worsnop, D. R., Kulmala, M., Kerminen, V.-M., and Petäjä, T.: Reactivity of stabilized Criegee intermediates (sCIs) from isoprene and monoterpene ozonolysis toward SO2 and organic acids, Atmos. Chem. Phys., 14, 12143–12153, doi:10.5194/acp-14-12143-2014, 2014.

Stark, H., Brown, S. S., Goldan, P. D., Aldener, M., Kuster, W. C., Jakoubek, R., Fehsenfeld, F. C., Meagher, J., Bates, T. S., and Ravishankara, A. R.: Influence of nitrate radical on the oxidation of dimethyl sulfide in a polluted marine environment, J. Geophys. Res., 112, D10S10, doi:10.1029/2006JD007669, 2007.

Stone, D., Blitz, M., Daubney, L., Ingham, T., and Seakins, P.: CH_2OO Criegee biradical yields following photolysis of CH_2I_2 in O_2, Phys. Chem. Chem. Phys., 15, 19119–19124, 2013.

Stone, D., Blitz, M., Daubney, L., Howes, N. U. M., and Seakins, P.: Kinetics of CH_2OO reactions with SO_2, NO_2, NO, H_2O, and CH_3CHO as a function of pressure, Phys. Chem. Chem. Phys., 16, 1139–1149, 2014.

Su, Y. -T., Lin, H. -Y., Putikam, R., Matsui, H., Lin, M. C., and Lee, Y.-P.: Extremely rapid self-reaction of the simplest Criegee intermediate CH_2OO and its implications in atmospheric chemistry, Nat. Chem., 6, 477–483, 2014.

Taatjes, C. A., Meloni, G., Selby, T. M., Trevitt, A. J., Osborn, D. L., Percival, C. J., and Shallcross, D. E.: Direct observation of the Gas-Phase Criegee Intermediate (CH_2OO), J. Am. Chem. Soc., 130, 11883–11885, 2008.

Taatjes, C. A., Welz, O., Eskola, A. J., Savee, J. D., Osborn, D. L., Lee, E. P. F., Dyke, J. M., Mok, D. W. K., Shallcross, D. E., and Percival, C. J.: Direct measurements of Criegee intermediate (CH_2OO) formed by reaction of CH_2I with O_2, Phys. Chem. Chem. Phys., 14, 10391–10400, 2012.

Taatjes, C. A., Welz, O., Eskola, A. J., Savee, J. D., Scheer, A. M., Shallcross, D. E., Rotavera, B., Lee, E. P. F., Dyke, J. M., Mok, D. K. W., Osborn, D. L., and Percival, C. J.: Direct Measurements of Conformer-Dependent Reactivity of the Criegee Intermediate CH_3CHOO, Science, 340, 177–180, 2013.

Vereecken, L., Harder, H., and Novelli, A.: The reaction of Criegee intermediates with NO, RO_2, and SO_2, and their fate in the atmosphere, Phys. Chem. Chem. Phys., 14, 14682–14695, 2012.

Vereecken, L., Harder, H., and Novelli, A.: The reactions of Criegee intermediates with alkenes, ozone and carbonyl oxides, Phys. Chem. Chem. Phys., 16, 4039–4049, 2014.

von Glasow, R., and Crutzen, P. J.: Tropospheric Halogen Chemistry, edited by: Holland, H. D. and Turekian, K. K., Treatise on Geochemistry Update 1, vol. 4.02, 1–67, 2007.

Wei, W., Zheng, R., Pan, Y., Wu, Y., Yang, F., and Hong, S.: Ozone Dissociation to Oxygen Affected by Criegee Intermediate, J. Phys. Chem. A, 118, 1644–1650, 2014.

Welz, O., Savee, J. D., Osborn, D. L., Vasu, S. S., Percival, C. J., Shallcross, D. E., and Taatjes, C. A.: Direct Kinetic Measurements of Criegee Intermediate (CH_2OO) Formed by Reaction of CH_2I with O_2, Science, 335, 204–207, 2012.

Welz, O., Eskola, A. J., Sheps, L., Rotavera, B., Savee, J. D., Scheer, A. M., Osborn, D. L., Lowe, D., Murray Booth, A., Xiao, P., Anwar H., Khan, M., Percival, C. J., Shallcross, D. E., and Taatjes, C. A.: Rate coefficients of C1 and C2 Criegee intermediate reactions with formic and acetic acid near the collision limit: direct kinetics measurements and atmospheric implications, Angew. Chem. Int. Ed. Engl., 53, 4547–4550, 2014.

Williams, J., Custer, T., Riede, H., Sander, R., Jöckel, P., Hoor, P., Pozzer, A., Wong-Zehnpfennig, S., Hosaynali Beygi, Z., Fischer, H., Gros, V., Colomb, A., Bonsang, B., Yassaa, N., Peeken, I., Atlas, E. L., Waluda, C. M., Van Ardenne, J. A., and Lelieveld,

J.: Assessing the effect of marine isoprene and ship emissions on ozone, using modelling and measurements from the South Atlantic Ocean, Environ. Chem., 7, 171–182, 2010.

Wingenter, O. W., Sive, B. C., Blake, N. J., Blake, D. R., and Rowland, F. S.: Atomic chlorine concentrations derived from ethane and hydroxyl measurements over the equatorial Pacific Ocean: Implication for dimethyl sulfide and bromine monoxide, J. Geophys. Res., 110, D20308, doi:10.1029/2005JD005875, 2005.

Yassaa, N., Peeken, I., Zöllner, E., Bluhm, K., Arnold, S., Spracklen, D., and Williams, J.: Evidence for marine production of monoterpenes, Environ. Chem., 5, 391–401, 2008.

Zhang, D., Lei, W., and Zhang, R.: Mechanism of OH formation from ozonolysis of isoprene: kinetics and product yield, Chem. Phys. Lett., 358, 171–179, 2002.